physica status solidi

Modeling the interface between crystalline silicon and silicon oxide polymorphs

Journal:	*physica status solidi*
Manuscript ID:	pssc.201200447
Wiley - Manuscript type:	Contributed Article
Date Submitted by the Author:	03-Jul-2012
Complete List of Authors:	Pivac, Branko ; R. Boskovic Institute, Materials Physics Kovacevic, Goran; R. Boskovic Institute, Material Physics
Keywords:	silicon, interface, structure , stability, molecular dynamics

SCHOLARONE™
Manuscripts

For Peer Review

pss-Header will be provided by the publisher

Review copy – not for distribution

(pss-logo will be inserted here by the publisher)

Modeling the interface between crystalline silicon and silicon oxide polymorphs

Goran Kovačević [*,1], **Branko Pivac** [**,1]

[1] Rudjer Boskovic Institute, POB 180, HR-10002 Zagreb, Croatia

Received ZZZ, revised ZZZ, accepted ZZZ
Published online ZZZ (Dates will be provided by the publisher.)

Keyword silicon, interface, structure, stability, molecular dynamics

* Corresponding author: e-mail gkova@irb.hr
** e-mail pivac@irb.hr, Phone: +00 385 1 4561068, Fax: +00 385 1 4680114

Structures of interfaces between crystalline silicon and several polymorphes of crystalline silicon oxides are modeled by molecular dynamics with Reax force field. Molecular dynamics and annealing procedures were conducted in order to create the most plausible interface structure. As the measure of stability of the interface, the energies of selected subsystems, are calculated. The interface between silicon and β-cristobalite turned out to have an amorphous arrangement of atoms. In all other interfaces, the crystalline order is preserved with defects in form of dislocated oxygen atoms. The interfaces between silicon and tridymite are the most ordered and energetically the most stable, but with the highest strain in the silicon layer.

Copyright line will be provided by the publisher

For Peer Review

1 Introduction

The interface between silicon and it's oxide is one of the most important atomic interfaces in materials used in manufacture of modern electronic devices [1]. Although it has been a subject of research for more than 30 years [2,3], it's structure is still unclear. While silicon, used in manufacture of electronic devices is crystalline, thermally grown SiO_2 is amorphous [4-7] and the interface is abrupt and smooth.[8] Nevertheless, there are indications about the ordered crystalline structure of the SiO_2 in the Si-SiO_2 interface layer. [9] β-cristobalite [10] and tridymite [3,8] structures have been reported experimentally. Different structures, obtained by different authors, can be attributed to different preparation conditions. [11] In addition to the experimental observations, several theoretical studies have been performed, and several models for SiO_2 layer have been established:

a) amorphous SiO_2 (aSiO_2) [4,12-15]
b) β-cristobalite (cSiO_2) [16-20]
c) tridymite (tSiO_2) [14,18-23]
d) α-quartz (αqSiO_2) [24,25]
e) β-quartz (βqSiO_2) [18,26]

Careful examination of possible arrangements of oxygen atoms on the (001) surface of silicon crystal has led to two possible ordered structures that remove dangling bonds on the silicon surface, leaving all silicon atoms "*valence-satisfied*". [18] In both structures, oxygen atom inserts in Si-Si bridges on the (001) silicon surface [27-29], however in one structure oxygen atoms are arranged in rows (stripe phase) and in another in checkerboard pattern (check phase).[14,18] These structures can be extended by adding SiO_2 layers to the Si(001) surface covered with one layer of oxygen. The checkerboard pattern can be extended to the quartz, cristobalite and β tridymite crystal structures, and the row pattern can be extended to the β tridymite crystal structure only. In addition to inserting oxygen to Si-Si bridges, several other options were found in the case of silicon-crystobalite (Si-cSiO_2) interface. This interface has an advantage over interfaces with quartz (qSiO_2) and β-cristobalite (cSiO_2), since the unit cell of the cSiO_2 matches the diagonal of the crystalline silicon unit cell. [16,30] Therefore, low strain interface can be created if the [100] direction in the cSiO_2 aligns with the [110] direction in silicon. Unsatisfied valencies of silicon atoms in the interface can be resolved by replacing these silicon atoms with oxy-

Copyright line will be provided by the publisher

gen atoms, or by introducing oxygen atoms bonded with these silicon atoms by double bonds. [16]

The reax force field [31-33] is one of the best force fields for describing systems subjected to chemical reactions. It is capable of describing systems on much wider parts of potential energy surface than conventional force fields. Reax force field parameters for silicon and silicon oxide systems [34-35] have been developed and their ability for describing equations of state for several polymorphs of silicon and silicon oxide proved [34]. In addition, the ability for using this force field in molecular dynamics (MD) simulations of silicon-silicon oxide interfaces was demonstrated.[34]

In this work, our aim is to investigate stability and structure of silicon-silicon oxide interface. Several crystalline forms of silicon oxide are considered: β-cristobalite, tridymite and β-quartz.

2 Theoretical methods

Model systems were created by inserting a slab of silicon atoms into the silicon oxide system. The dimensions of the unit cell of the silicon oxide were adjusted in order to match the dimension of the silicon unit cell. A care was taken that all atoms in the interfaces are in proper positions and bonding between atoms in different layers is correct. Additional oxygen atoms are inserted in the interface layer to satisfy valencies of all silicon atoms that were left undercoordinated. The unit cell was subjected to series of geometry optimization and low temperature MD steps in order to remove strain from the system. After relaxation, the temperature of the quartz layers was increased to 1000 K over 15 ps. The temperature of 1000 K is too low for melting the silicon or any of silicon oxide forms considered, but is high enough for atom rearrangements to take place in the $Si\text{-}SiO_2$ interface region. The MD simulation was performed on the system for 50 ps after which, the system was annealed for another 50 ps at the cooling rate of $1.94\cdot10^{13}$ K/s. Geometry optimization was performed on the final geometry. It was shown [4] that the annealing procedure leads to structures that are more similar to structures, optimized with DFT. Periodic boundary conditions were applied in all three dimensions. The time integration step of 0.5 fs was used with the velocity-Verlet integrator in all MD steps. The temperature and the pressure were kept with the Nose-Hoover thermostat/barostat. The pressure of 1 atmosphere was kept in all MD steps. All MD calculations were done with the LAMMPS program package.[36] Charges, used in the reax force field for calculation of energy were extracted in order to characterize atom bonding in the silicon-silicon oxide interfaces. Systems consisting of only Si, $c\text{-}SiO_2$, t- SiO_2 and $\beta q\text{-}SiO_2$ were also subjected to molecular dynamics and optimization in order to compare their structures with the structures from interfaced systems. Atoms from the representative subsystems, consisting of atoms that constitute the interfaces are selected. The subsystems are defined by the upper and lower boundaries (along z coordinate) that were defined by layers of silicon atoms that are in oxidation state +4 (boundary towards SiO_2) and in oxidation state 0 (boundary towards silicon). Other boundaries are stochastically varied in order to create subsystems with equal number of atoms, bonds and valence angles. The energy of these subsystems (E_{system}) are calculated by using equation 1:

$$E_{system} = \sum_{i}^{bonds} E_{bond,i} + \sum_{i}^{angles} E_{val,i} + \sum_{i}^{atoms} \left\{ E_{\text{over},i} + E_{under,i} + E_{lp,i} + \sum_{j\neq i}^{atoms} \left[E_{vdWaals,i,j} + E_{Coulomb,i,j} \right] \right\} \quad (1)$$

where the individual contributions are: bond energies (E_{bond}), valence angle energies (E_{val}), overcordination energy term (E_{over}), undercoordination energy term (E_{under}), lone pair energy term (E_{lp}), penalty energy (E_{pen}), conjugation energy (E_{conj}), Van der Waals energy ($E_{vdWaals}$) and Coulomb energy ($E_{Coulomb}$). Torsion energy, conjugation energy and energy penalty terms are not referenced since in the Reax force field for silicon-silicon oxide systems torsion is described with non-bonding interactions and conjugation and penalty energy contributions are negligible. [34] The individual energy terms that were used for calculation of the subsystem energy in equation (1) are the same energy contributions that were used for calculation of energies of $SiO_2\text{-}Si\text{-}SiO_2$ *systems. In that* way the comparable energies of interfaces were calculated.

3 Results and discussion

Five models for silicon-silicon oxide interfaces were considered; two models for $cSiO_2\text{-}Si$ and $tSiO_2\text{-}Si$ interfaces, and one for $qSiO_2\text{-}Si$ interface. Dangling bonds in the $cSiO_2\text{-}Si$ interface were eliminated according to Wagner at al. [16] with the “bridge oxygen model” (BOM) or the “double bond model” (DBM) as seen on figures 1a and 1b. The row (R) and the checkerboard pattern (CB) are used for arrangement of oxygen atoms [14,18] in the $tSiO_2\text{-}Si$ interfaces. That oxygen atoms define Si-O-Si bridges. (Figures 1c – 1f) Only the β polymorph of quartz is considered (figures 1g and 1h) since the $\beta qSiO_2$ is a high temperature polymorph of the $\alpha qSiO_2$ and the barrier for their conversion is very low. Only the row pattern of oxygen atoms is possible in the $Si\text{-}\beta qSiO_2$ interface.

For Peer Review

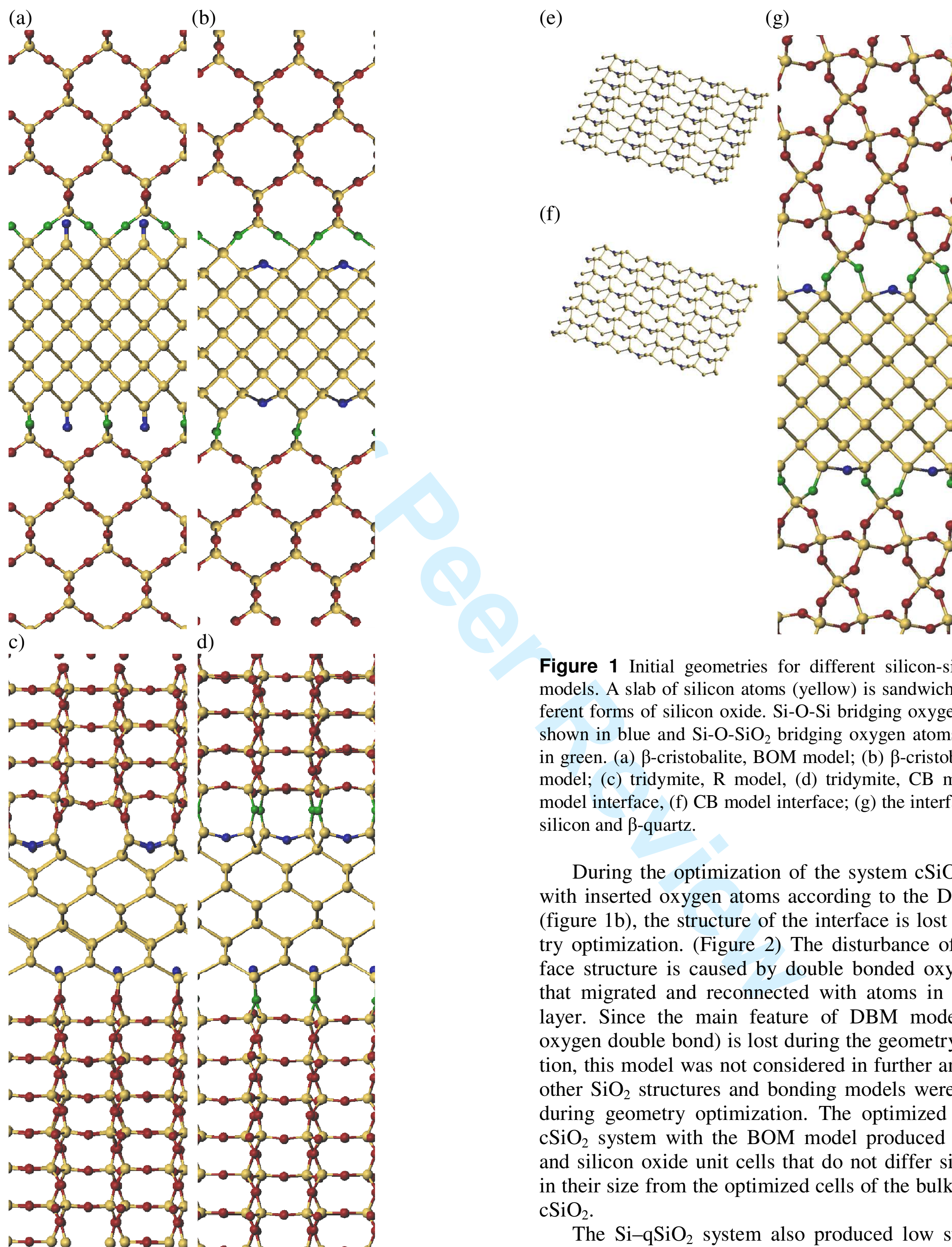

Figure 1 Initial geometries for different silicon-silicon oxide models. A slab of silicon atoms (yellow) is sandwiched with different forms of silicon oxide. Si-O-Si bridging oxygen atoms are shown in blue and Si-O-SiO_2 bridging oxygen atoms are shown in green. (a) β-cristobalite, BOM model; (b) β-cristobalite, DBM model; (c) tridymite, R model, (d) tridymite, CB model. (e) R model interface, (f) CB model interface; (g) the interface between silicon and β-quartz.

During the optimization of the system $cSiO_2$-Si-$cSiO_2$ with inserted oxygen atoms according to the DBM model (figure 1b), the structure of the interface is lost by geometry optimization. (Figure 2) The disturbance of the interface structure is caused by double bonded oxygen atoms that migrated and reconnected with atoms in the silicon layer. Since the main feature of DBM model (silicon-oxygen double bond) is lost during the geometry optimization, this model was not considered in further analysis. All other SiO_2 structures and bonding models were preserved during geometry optimization. The optimized $cSiO_2$–Si–$cSiO_2$ system with the BOM model produced the silicon and silicon oxide unit cells that do not differ significantly in their size from the optimized cells of the bulk Si and the $cSiO_2$.

The Si–$qSiO_2$ system also produced low strain interface since the change in cell dimensions is less than 5%. The Si–$tSiO_2$ interfaces (R and CB models) are strained since the silicon unit cell have to be elongated for about 12% in *x* and *y* direction in order to make the interface with $tSiO_2$. The $tSiO_2$ didn't change dimension significant-

Copyright line will be provided by the publisher

ly, since in our model the slab of $tSiO_2$ is much thicker than the slab of the Si and in that case the $tSiO_2$ layer determines the inter-atomic separations.

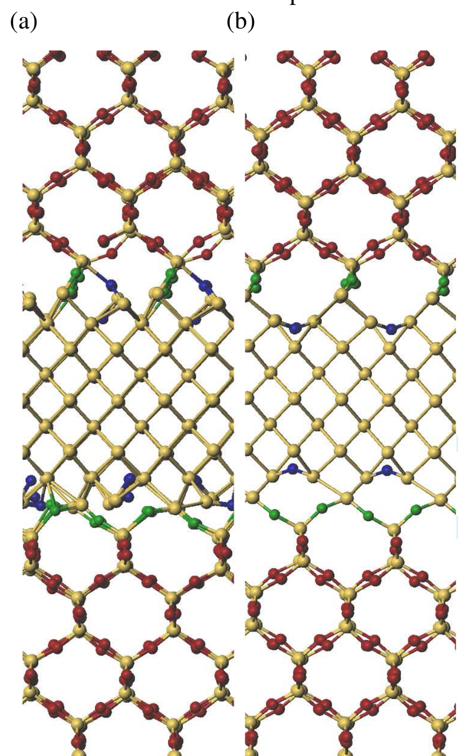

Figure 2 Optimized silicon slab, sandwiched in $cSiO_2$. (a) Interface between Si and $cSiO_2$, modeled according to the DBM model. (b) Interface between Si and c-SiO_2, modeled according to the BOM model.

During annealing of systems, some of oxygen atoms entered the silicon layer. (Figure 3) These oxygen atoms came from the interface layer, either from the Si-O-Si bridging positions, or from the Si-O-SiO_2 bridging positions. In most cases Si-Si bond is formed if the oxygen atom from the bridging position dislocates into the Si slab. The number of dislocated oxygen atoms in the Si-$tSiO_2$ system is surprisingly low considering that the Si-$tSiO_2$ interface is strained. The greatest change in structure, during heating and annealing is in the Si-$cSiO_2$ interface where Si-O-SiO_2 bridges are completely reorganized into the amorphous SiO_2 layer. In all other interfaces the crystalline order is preserved. The disordered structure can be seen in the atom charge distribution along the direction, perpendicular to the interfaces (*z* coordinate, Figure 4). Atomic charges, used in the Reax force field are evaluated by electron equilibration method [37] and we used them as a convenient indicator for distribution of silicon atoms with different oxidation numbers. While in ordered interfaces the charges of silicon atoms change stepwise, from the crystalline silicon to the silicon oxides, in the case of amorphous interface, there is a continuous change. The stepwise change in charges (in the case of ordered interfaces) is the consequence of the presence of silicon atoms in intermediate oxidation states. The dislocated oxygen atoms cause change in oxidation states of silicon atoms outside of the layer of silicon atoms with the same oxidation number. Also, the strain in the interfaces reflects in the systematic change in silicon (IV) and oxygen charges near the interface.

Summed energies of bonds, valence angles, local atomic contributions and long range interactions in the limited region in interfaces are provided as a measure of stability of these interfaces. (Table 1) Since the number of atoms, bonds and valence angles is equal in all selected interface models, the energies, shown in Table 1 can be used to estimate the stability of the interface without the influence of the Si and SiO_2 layers. The most stable interface turned out to be the interface between silicon and $tSiO_2$. In that interface, coordination of all atoms is close to ideal and only difference from the initial interface (Figure 1d) is in oxygen atoms that are dislocated and inserted into Si-Si bonds. The interface between silicon and $\beta cSiO_2$ is characterized by appearance of tri-coordinated oxygen atoms.

Although most of the bonding defects are present in interfaces, the energy of the interface *per se* can't give information about the strain in the interface since a great amount of deformation is present in the layers of silicon and silicon oxide. The strain in the interface can be characterized by observing change in internal coordinates and comparing it with values in non-stressed, ideal crystalline silicon and silicon oxides. Figure (5) shows bond lengths in modeled systems as a function of *z* coordinate. The uninterfaced crystals of silicon and all considered silicon oxides are subjected to same geometry optimization and molecular dynamics steps as Si-SiO_2-Si models in order to obtain bond lengths characteristic for that crystals. The difference between bond lengths in cristalline tridymite and β-quartz that are interfaced with silicon with respect to uninterfaced structures is unsignificant. The crystalline structure of β-cristobalite is disordered despite the annealing to below 20 K and geometry optimization. In all cases there is a large disorder in silicon-silicon bond lengths near the interface that is caused by irregularities in crystalline structure, due to dislocated oxygen atoms. In addition to the disorder in Si-Si bond lengths, in the case of β-tridymite, there is a systematic increase in Si-Si bond-length through the entire slab. That increase is a consequence of mismatch in the unit cell dimensions, although most of the strain in initial structures is removed with the geometry optimizations and molecular dynamics. In the silicon slab, sandwiched by β-cristobalite, there is a trend in increasing bond lengths from the center of the slab toward the interface.

Copyright line will be provided by the publisher

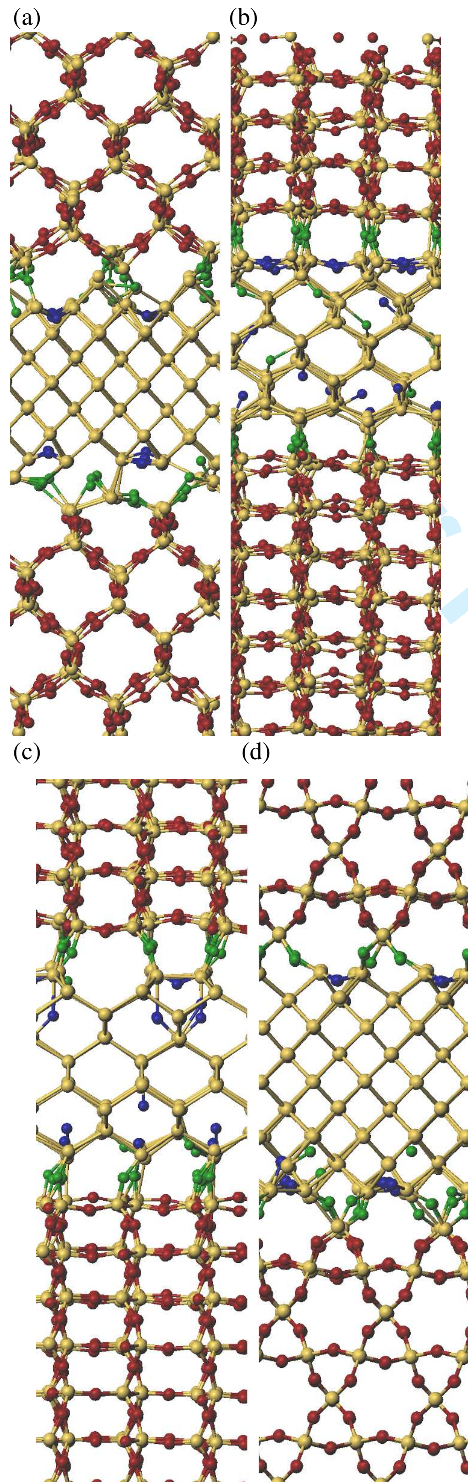

Figure 3 Structures of the SiO_2-Si-SiO_2 interfaces after thermal treatment and annealing. Oxygen atoms that were originally in the Si-O-Si bridging position were shown in blue color and oxygen atoms that were part of Si-O-SiO_2 bridges are shown in green color. (a) $cSiO_2$ BOM model, (b) $tSiO_2$ CB model (c) $tSiO_2$ R model, (d) $qSiO_2$

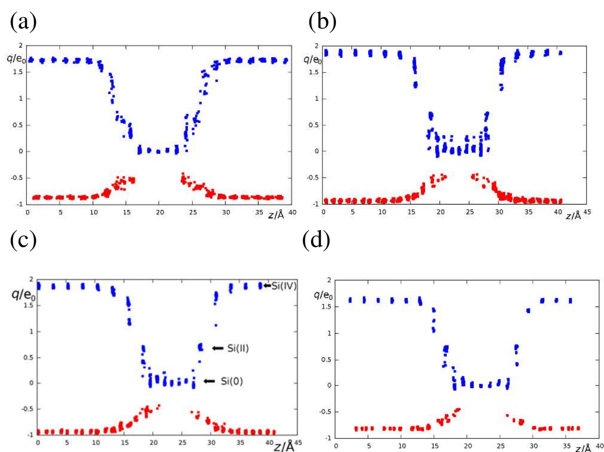

Figure 4 Charges of atoms as a function of their z coordinate.

The appearance of tri-coordinated oxygen atoms have been observed in silicon-silicon oxide interface, by using the first-principles molecular dynamics simulation. [12] Relatively large number of oxygen atoms in the interface and relatively large number of strained bonds and valence angles makes this interface energetically unfavorable.

Table 1 Energies (E_{system}) of interfaces inside the SiO_2-Si-SiO_2 systems.

Interface	Size /Å	E_{system}/kcal mol^{-1}
Si-cSiO_2 BOM	11.0 × 11.0 × 4.9	-10950.27
Si-tSiO_2 CB	11.9 × 11.0 × 4.4	-12890.25
Si-tSiO_2 R	9.7 × 11.0 × 5.6	-12271.46
Si-qSiO_2	14.0 × 11.0 × 4.1	-11688.85

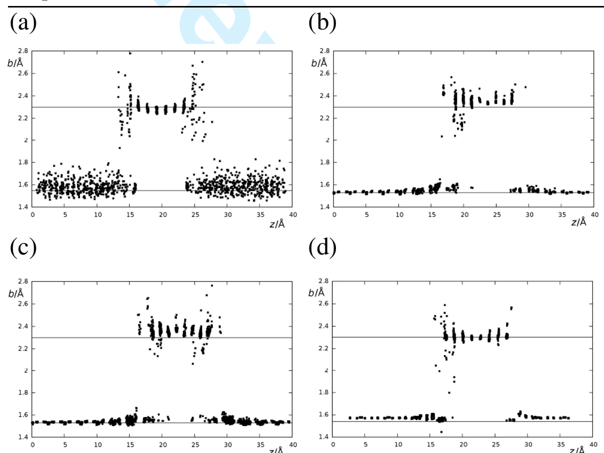

Figure 5 Bond lengths as a function of z coordinate. Si-Si bond lengths in silicon crystal are indicated by the upper horizontal line, and Si-O bond length in corresponding silicon oxide is indicated

For Peer Review

by lower horizontal line. (a) $cSiO_2$ BOM model, (b) $tSiO_2$ CB model (c) $tSiO_2$ R model, (d) $qSiO_2$

3 Conclusion

The DBM model of the interface between crystalline silicon and crystalline β-cristobalite was proved as unstable. The BOM model of the same interface leads to the layer of atoms with amorphous structure, while the interfaces between crystalline silicon and quartz, and tridymite remain crystalline after annealing with molecular dynamics with Reax force field. The local strain in the Si-SiO_2 interface can be resolved by migration of oxygen atoms to the Si-Si bonds in the silicon layer. The interfaces Si-$cSiO_2$ are the most ordered and energetically the most stable, but with the highest strain in the silicon layer.

Acknowledgements We are grateful to Adri van Duin for supplying us the Reax force field parameters. Computations in this work has been done in the Croatian national grid infrastructure (Cro-Ngi). This study has been partially funded by EU project NanoPV (FP7-NMP3-SL-2011-246331).

References

[1] G. D. Wilk, R. M. Wallace, J. M. Anthony, J. Appl. Phys. **89,** 5243 (2001)
[2] M. M. Banaszak Holl, F. R. McFeely, Phys. Rev. Lett. **71**, 2441 (1993)
[3] A Pasquarello, M. S. Hybertsen, R. Car, Phys. Rev. Lett. **74**, 1024 (1995)
[4] R. M. Van Ginhoven, H.P. Hjalmarson, Nucl. Instr. and Meth. in Phys. Res. B **255**, 183 (2007)
[5] A. C. Diebold, D. Venables, Y. Chabal, D. Muller, M. Weldon, E. Garfunkel, Mat. Sci. Semic. Proc. **2**, 103 (1999)
[6] H. Akatsu, Y. Sumi, I. Ohdomari, Phys. Rev. B **44**, 1616 (1991)
[7] N. Nagasima, Jpn. J. Appl. Phys. **9**, 879 (1970)
[8] A. Ourmazd, D. W. Taylor, J. A. Rentschler, Phys. Rev. Lett. **59**, 213 (1987)
[9] A. Munkholm, S. Brennan, F. Comin, L. Ortega, Phys. Rev. Lett. **75**, 4254 (1995)
[10] I Takahashi, T Shimura and J Harada, J. Phys. Condens. Mater, **5**, 6525 (1993)
[11] F. J. Himpsel, F. R. McFeely, A. Taleb-Ibrahimi, J. A. Yarmoff, G. Hollinger, Phys. Rev. B **38**, 6084 (1988)
[12] A. Pasquarello, M. S. Hybertsen R. Car, Nature, **396**, 58 (1998)
[13] K.-O. Ng D. Vanderbilt, Phys. Rev. B **59**, 132 (1999)
[14] Y. Tu, J. Tersoff, Phys. Rev. Lett. **84**, 4393 (2000)
[15] N. Nagashima, Jpn. J. Appl. Phys. **9**, 879 (1970)
[16] J.-M. Wagner, K. Seino, F. Bechstedt, A. Dymiati, J. Mayer, R. Rölver, M. Först, B. Berghoff, B. Spangenberg, H. Kurz, J. Vac. Sci. Technol. A **25**, 1500 (2007)
[17] E. Degoli, S. Ossicini, Surf. Sci. **470**, 32 (2000)
[18] R. Buczko, S. J. Pennycook, S. T. Pantelides, Phys. Rev. Lett. **84**, 943 (2000)
[19] T. Yamasaki, C. Kaneta, T. Uchiyama, T. Uda, K. Terakura Phys. Rev. B **63**, 115314 (2001)
[20] A. Pasquarello, M. S. Hybertsen, R. Car, Phys. Rev. B **53**, 10942 (1996)
[21] T. A. Kirichenko, D. Yu, S. K. Banerjee, G. S. Hwang Phys. Rev. B **72**, 035345 (2005)
[22] A. Stirling, A. Pasquarello, J.-C. Charlier, R. Car, Phys. Rev. Lett. **85**, 2773 (2000)
[23] A. Pasquarello, M. S. Hybertsen, R. Car, Appl. Phys. Lett. **68**, 625 (1996)
[24] K. Kutsuki, T. Ono, K. Hirose, Sci. Technol. Adv. Mater. **8**, 204 (2007)
[25] T. Yamasaki, C. Kaneta, T. Uchiyama, T. Uda, K. Terakura, Phys. Rev. B **63**, 115314 (2001)
[26] H, Kageshima K. Shiraishi, Phys. Rev. Lett. **81**, 5936 (1998)
[27] Y. Miyamoto A. Oshiyama, Phys. Rev. B, **41**, 12680 (1990)
[28] T. Hoshino, M. Tsuda, S. Oikawa, I. Ohdomari, Phys. Rev. B **50**, 14999 (1994)
[29] A. Stirling, A. Pasquarello, J.-C. Charlier, R. Car, Phys. Rev. Lett. **85** (2000) 2773-2776
[30] I. Takahashi, T. Shimura J. Harada, J. Phys.: Condens. Matter **5**, 6525 (1993)
[31] A. C. T. van Duin, S. Dasgupta, F. Lorant, W. A. Goddard III, J. Phys. Chem. A **105**, 9396 (2001)
[32] K. Chenoweth, A. C. T. van Duin, W. A. Goddard III, J. Phys. Chem. A **112**, 1040 (2008)
[33] M. J. Buehler, A. C. T. van Duin, W. A. Goddard III Phys. Rev. Lett. **96**, 095505 (2006)
[34] A. C. T. van Duin, A. Strachan, S. Stewman, Q. Zhang, X. Xu, W. A. Goddard III, J. Phys. Chem. A **107**, 3803 (2003)
[35] J. C. Fogary, H. M. Aktulga, A, Y. Grama, A. C. T. van Duin, S. A. Pandit, J. Chem. Phys. **132**, 174704 (2010)
[36] S. Plimpton, J Comp. Phys., **117**, 1 (1995)
[37] W. J. Mortier, S. K. Ghosh, S. Shankar, J. Am. Chem. Soc. *108*, 4315 (1986)

For Peer Review

Copyright line will be provided by the publisher